PALEOCEANOGRAPHY, VOL. 24, PA4213, doi:10.1029/2008PA001702, 2009



# Nitrogen isotopic evidence for deglacial changes in nutrient supply in the eastern equatorial Pacific

R. S. Robinson,[1] P. Martinez,[2] L. D. Pena,[3] and I. Cacho[3]

Received 14 October 2008; revised 14 September 2009; accepted 18 September 2009; published 15 December 2009.

[1] The Eastern Equatorial Pacific (EEP) is a high nutrient–low chlorophyll region of the ocean. Downcore nitrogen isotope records from the EEP have been previously interpreted as a direct reflection of changes in nutrient consumption. However, the observed changes in sedimentary $\delta^{15}$N since the last glacial maximum have no coherent relationship with export productivity or an inferred variation in the iron-to-nitrate ratio of the surface waters. Rather, downcore N isotope records in the EEP strongly resemble changes in the extent of water column denitrification as recorded in nearby sedimentary $\delta^{15}$N records along the western margin of the Americas. This similarity is attributed to the overprinting of the N isotopic composition of nitrate in the EEP through the advection of nitrate westward from the margins in the subsurface. A local nitrogen isotope record of changes in the degree of nutrient consumption is extracted from the bulk sedimentary record by subtracting two different sedimentary $\delta^{15}$N records of denitrification changes from two new EEP $\delta^{15}$N records (TR163-22 and ODP Site 1240). The denitrification records used are from 1) the Central American margin (ODP Site 1242) and 2) the South American margin (GeoB7139-2). The degree of consumption in the surface waters declines rapidly from elevated values during the last glacial maximum to a pair of minima around 15 and 11–13 ka, and finally it increases into the Holocene. The derived EEP nitrogen isotope record indicates that the regional peak in export productivity occurred when the supply of nutrients exceeded the apparently high demand. The influx of nutrients during the deglaciation is attributed to the resumption of intense overturning in the Southern Ocean and the release of sequestered $CO_2$ and nutrient-rich, $O_2$ poor waters from the deep ocean. This has important implications for understanding the glacial-interglacial scale variation in intermediate water suboxia and water column denitrification.

**Citation:** Robinson, R. S., P. Martinez, L. D. Pena, and I. Cacho (2009), Nitrogen isotopic evidence for deglacial changes in nutrient supply in the eastern equatorial Pacific, *Paleoceanography*, *24*, PA4213, doi:10.1029/2008PA001702.

## 1. Introduction

[2] The eastern tropical Pacific (ETP), defined as the oceanic region between 23.5°N and 23.5°S and between 140°W and the Americas, houses both the equatorial and coastal upwelling systems. It is responsible for approximately 10% of global ocean productivity [*Pennington et al.*, 2006]. The ETP also houses two large regions of water column denitrification, the bacterial reduction of nitrate under low oxygen conditions, in the subsurface beneath the marginal upwelling systems. A significant fraction of the total fixed nitrogen in the ocean is removed within these waters. The suboxic conditions along the margins in the ETP are potentially regulated in part by the biogeochemical conditions at the equator, where large export fluxes associated with the EEP upwelling system are responsible for the drawdown in subsurface oxygen concentrations in the Equatorial Undercurrent (EUC) [*Lukas*, 1986]. The low oxygen EUC in the easternmost EEP feeds into the poleward undercurrents, the California Undercurrent and the Peru-Chile Undercurrent, that flow through the large regions of open ocean suboxia in the ETP.

[3] The glacial-interglacial climate cycles are imprinted on biogeochemical changes recorded in the sediments of the ETP. Variations in nutrient supply, export productivity and water column denitrification are related to both this regional interplay of biological and physical processes [*Toggweiler et al.*, 1991] and to remote, global scale climate [*Lea et al.*, 2006], circulation [*M. Kienast et al.*, 2006; *Meissner et al.*, 2005; *Toggweiler et al.*, 1991], and biogeochemical [*Loubere et al.*, 2007; *Robinson et al.*, 2007; *Spero and Lea*, 2002] changes. The best available estimates of export productivity, from $^{230}$Thorium ($^{230}$Th) normalized accumulation rate measurements, present a coherent pattern of change throughout the EEP since the last ice age. During the last 35ky, the interval of highest total organic carbon accumulation in the EEP, occurs during the deglaciation [*M. Kienast et al.*, 2006; *Kienast et al.*, 2007]. The deglacial peak in export also corresponds to a peak in the inferred nutrient content of the waters, based on planktonic foraminiferal $\delta^{13}$C [*Pena et al.*, 2008; *Spero and Lea*, 2002]. On the other hand, nitrogen isotope records from the region show a distinctly different sense of change, with a maximum in $^{15}$N/$^{14}$N (as $\delta^{15}$N) of sedimentary organic matter during the

[1]Graduate School of Oceanography, University of Rhode Island, Narragansett, Rhode Island, USA.
[2]EPOC, UMR 5805, Université Bordeaux 1, CNRS, Talence, France.
[3]GRC Geociències Marines, Department of Stratigraphy, Paleontology and Marine Geosciences, University of Barcelona, Barcelona, Spain.


0883-8305/09/2008PA001702$12.00

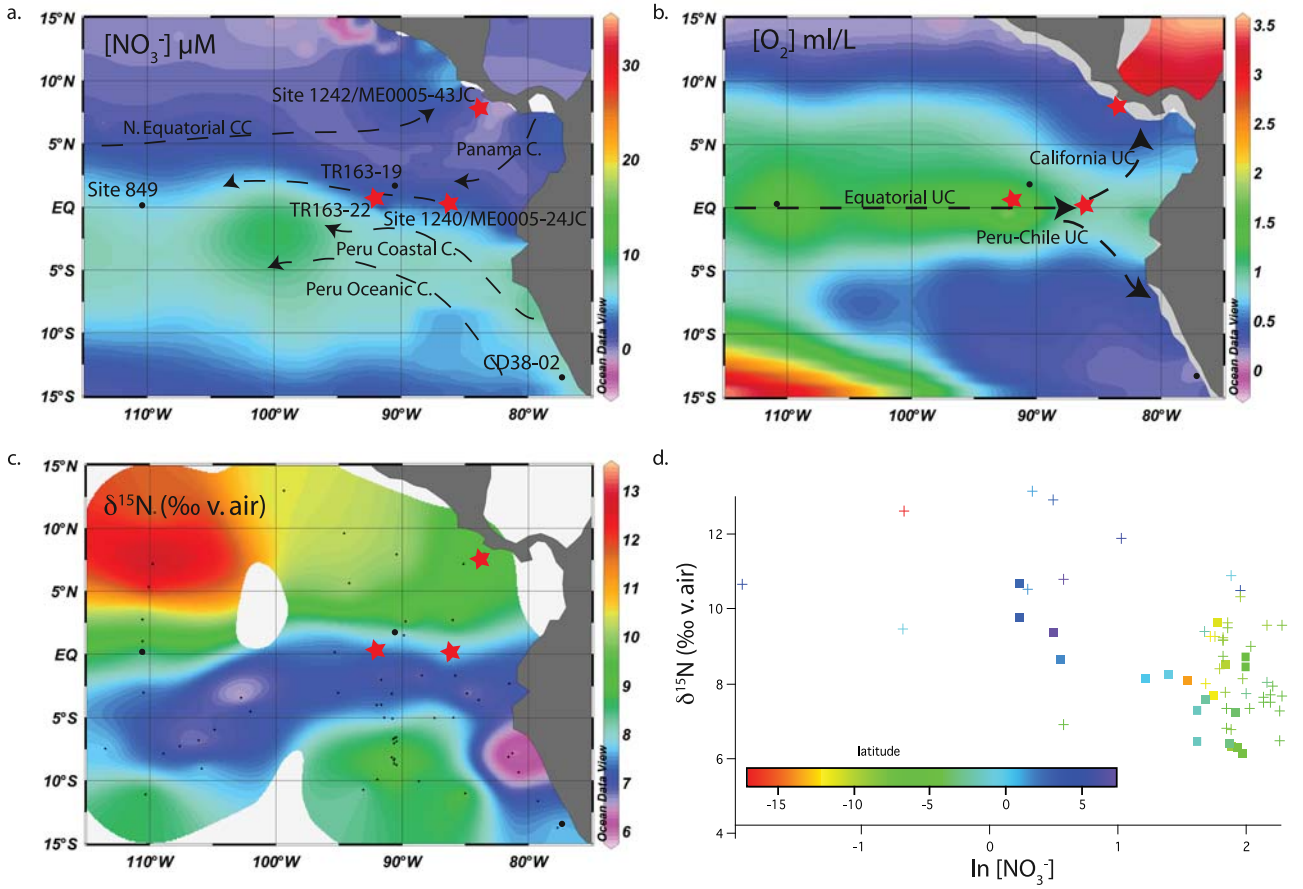


**Figure 1.** Surface ocean (a) $[NO_3^-]$ ($\mu$M) in the EEP [*Garcia et al.*, 2006b], (b) $[O_2]$ (ml/L) at 250 m depth [*Garcia et al.*, 2006a], (c) surface sedimentary $\delta^{15}N$ [*Farrell et al.*, 1995], and (d) $\delta^{15}N$ versus ln $[NO_3^-]$. Locations of Site 1240/ME0005-24JC, Site 1242/ME0005-43JC, and TR163-22 are marked with stars. Additional sites referenced in the text, ODP Site 849, TR163-19, and CD38-02, are marked with solid circles. Core site locations are marked on each map for reference to surface, subsurface, and surface sediment properties. Important surface ocean currents are drawn on the surface nitrate map (Figure 1a) while subsurface currents are shown in the 250m depth oxygen map (Figure 1b). All points in the $\delta^{15}N$ versus ln $[NO_3^-]$ plot are color coded as a function of latitude. The solid squares show sites located between 90°W and the margin of the Americas. The crosses show all samples west of 90°W.

deglaciation that was interpreted as a decrease in supply relative to demand [*Farrell et al.*, 1995]. Demand, or export, was based on total organic carbon ($C_{org}$) concentrations in the same cores [*Farrell et al.*, 1995]. In this nutrient replete system, the $\delta^{15}N$ of the sinking organic fraction should reflect the isotopic composition of the source nitrate and the degree of nutrient consumption due to the fractionation associated with the uptake and assimilation of nitrate. *Farrell et al.* [1995] assumed that there were no changes in the $\delta^{15}N$ of the source nitrate and attributed the signal entirely to changes in nutrient consumption.

[4] Their interpretation is largely based on the observed distribution of bulk $\delta^{15}N$ in the surface sediments in the EEP. Sedimentary $\delta^{15}N$ increases with decreasing nitrate concentrations in the surface ocean [*Farrell et al.*, 1995] (Figure 1). During the uptake and assimilation of nitrogen, phytoplankton incorporate $^{14}N$ nitrate at a higher rate than $^{15}N$ nitrate. The $\delta^{15}N$ of the remaining nitrate pool increases with increasing consumption and decreasing nitrate concentration and the $\delta^{15}N$ of the resulting organic matter increases in parallel, although offset to lower values as result of this fractionation. In the EEP, newly upwelled nitrate is progressively consumed as it is carried away from the equator by the trade wind driven divergence so that the $\delta^{15}N$ of nitrate and sedimentary N increase to the north and south of the equator (Figure 1c). The observed asymmetry in surface ocean nitrate concentrations is mirrored in the *Farrell et al.* [1995] map of surface sedimentary $\delta^{15}N$ (Figure 1).

[5] However, upon careful inspection of Farrell's downcore data from the EEP, the variation in $C_{org}$ concentration does not directly relate to the variation in $\delta^{15}N$, making a simple utilization interpretation difficult. $C_{org}$ is likely an adequate estimate of export production, as it is quite similar to the $^{230}Th$-normalized $C_{org}$ accumulation rate (AR)

records of *Kienast et al.* [2007]. More importantly, perhaps, the pattern of change in the EEP N isotope data is quite similar to the large glacial interglacial scale variation in $\delta^{15}$N recorded in the sediments underlying and downstream from the large regions of water column denitrification in the ETP [*Altabet et al.*, 1995, 2002; *De Pol-Holz et al.*, 2007; *Ganeshram et al.*, 2000; *Hendy et al.*, 2004; *Kienast et al.*, 2002; *Robinson et al.*, 2007]. This paper revisits the nitrogen isotope records of the EEP in the context of updated estimates of export productivity and variation in regional subsurface $\delta^{15}$N of nitrate with the goal of understanding or reconciling them with the existing carbon isotope data.

## 2. Background

[6] At the Pacific basin scale, the thermocline shoals toward the east to the point that it nearly intersects the surface in the far EEP. Strong southeasterly trades carry the South Equatorial Current (SEC) across the geographic equator. Opposing Coriolis forcing across the equator results in the divergence of the SEC surface waters to the north and south of the equator and the upwelling of relatively nutrient-rich subsurface water that fuels high rates of export production. In the subsurface, the Equatorial Undercurrent (EUC) delivers oxygen-rich water to the subsurface in the east, splitting two low oxygen tongues that originate along the margins and extend across the Pacific in the subsurface on either side of the EUC, perhaps as a sort of subsurface expression of the SEC (Figure 1b) [*Kessler*, 2006]. The EUC is split at the Galapagos Islands and largely deflected southwards to become the Peru-Chile Undercurrent [*Lukas*, 1986]. A smaller fraction is deflected north to join the California Undercurrent.

[7] The surface nitrate map shows a continuous pool of nitrate-rich water that extends from the Peru margin westward to approximately 140°W in the central equatorial Pacific (Figure 1a). The entire nitrate tongue is slightly offset to the south of the equator. The asymmetry is sometimes attributed to the advection of cool, nutrient-rich waters by the SEC from offshore Peru [*Fiedler and Talley*, 2006; *Toggweiler et al.*, 1991]. However, ADCP data show no clear evidence for direct flow from the Peru-Chile Current into the SEC [*Kessler*, 2006]. Seasonal nitrate and temperature variations indicate that the two regions are two separate upwelling systems. Only a ~1 month lag exists between temperature minima offshore Peru and those in the SEC, too short an interval to be attributed to advection [*Kessler*, 2006]. An alternative explanation for the asymmetrical surface nutrient maximum and temperature minimum exists. Small vertical circulation cells with a north-south trending axis are associated with the southerly cross-equatorial winds. Surface flow toward the north is balanced by southerly subsurface flow, resulting in enhanced upwelling to the south of the equator in the EEP [*Kessler*, 2006]. Another, biophysical, explanation was proposed based on an ecosystem model [*Toggweiler and Carson*, 1995]. The Fe-limited equatorial region is dominated by nannoplankton that prefer ammonium to nitrate and ammonium appears to be rapidly recycled. The result is a long residence time for nitrate within the equatorial system. The surface nitrate maximum is considered an expression of the subsurface build up nitrate. In the model, the advection of low-nitrate waters in from the west on and to the north of the equator, via the EUC and the north equatorial counter current (NECC), dilutes the nitrate pool north of the equator and causes the asymmetry in the nitrate concentrations [*Toggweiler and Carson*, 1995]. In addition, the modeled nitrate budget does not balance within the EEP. Nitrogen export is significantly less than inputs. The ecosystem model requires exchange between the EEP and the marginal upwelling systems for removal of nitrate via water column denitrification in the subsurface. Exchange is likely associated with the small meridional circulation cells [*Kessler*, 2006] and incorporation of partially denitrified waters from offshore Peru into the vertical circulation. The described circulation associated with the high nitrate tongue plays a central role in our interpretation of downcore N isotope records in the EEP.

## 3. Materials and Methods

### 3.1. Core Descriptions

[8] We report new bulk sedimentary nitrogen isotope and total nitrogen concentration data from ODP Sites 1240 (0.2°N, 86°W), drilled in a small abyssal valley north of Carnegie Ridge at 2921 m water depth in the Panama Basin [*Mix et al.*, 2003] and 1242 (7.5°N, 83.4°W) drilled beneath the Costa Rica dome on the northeastern edge of the Panama Basin on the Central American margin at 1364 m water depth [*Mix et al.*, 2003], and core TR163-22 (0.5°N, 92.3°W) recovered just west of the Galapagos Islands from 2830 m water depth (Figure 1). Annual mean surface nitrate concentrations are 0–1 $\mu$M at Site 1242 and ~3 $\mu$M at Site 1240 and TR163-22 [*Garcia et al.*, 2006b]. The equatorial sediments are carbonate ooze while the hemipelagic sediments at Site 1242 are composed of silty clays with minor amounts of well-preserved biogenic components [*Mix et al.*, 2003].

### 3.2. Age Models

[9] Sediment ages at both Site 1240 and TR163-22 were established using accelerator mass spectrometry (AMS) $^{14}$C dates from monospecific samples of *N. dutertrei*, the dominant planktonic foraminifera in Equatorial Pacific sediments [*Lea et al.*, 2006]. A marine reservoir age difference ($\Delta$R) of 72 ± 35 years was used by both *Pena et al.* [2008] and *Lea et al.* [2006] for Site 1240 and TR 163-22, respectively. Sediment ages at Site 1242 are from *Benway et al.* [2006]. They were determined by correlation of stable isotope, Mg/Ca, and sediment density records to colocated site ME0005-43JC for which an age model based on AMS $^{14}$C dates from mixed benthic foraminifera and oxygen isotope stratigraphy has been established [*Benway et al.*, 2006]. Sedimentation rates at Site 1242 averaged ~10cm/ky over the last 30ky. On the equator, sedimentation rates averaged ~15 cm/ky at Site 1240, due to high biogenic fluxes, while they were slightly lower at TR163-22, averaging ~9 cm/ky. An intercomparison between Mg/Ca and $\delta^{18}$O *G. ruber* records from TR163-22 and Site 1240 demonstrates a consistent chronological framework for the last 25 kyr with some minor offsets for the older interval of

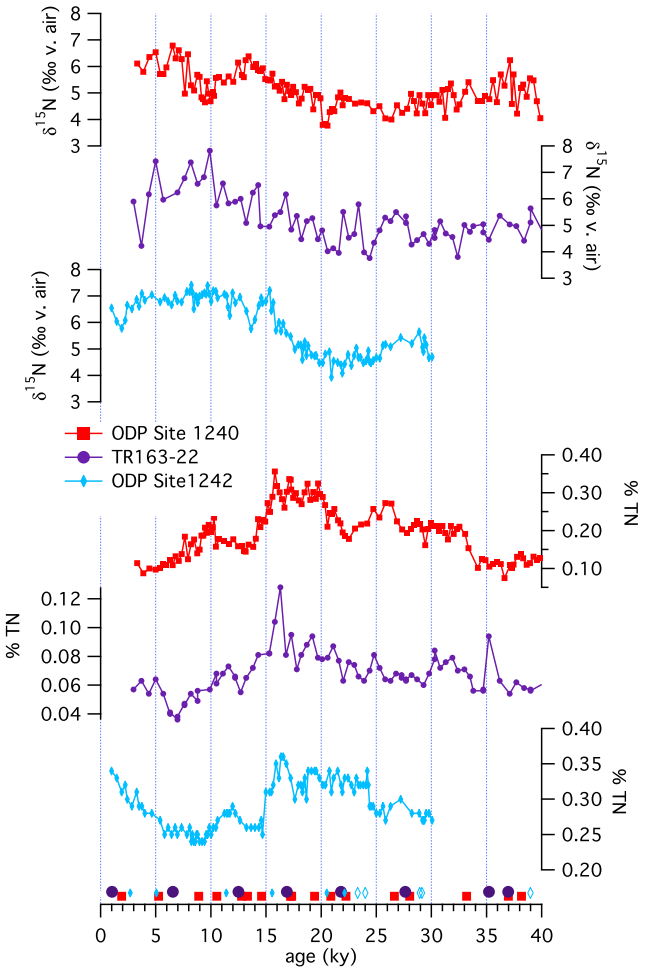


**Figure 2.** Downcore profiles of %TN and $\delta^{15}$N at Site 1240 (red squares), TR163-22 (purple circles), and Site 1242 (blue diamonds). Note the differences in the axis scales for TN. Age control points are illustrated at the bottom of the plot for Site 1240 (squares [*Pena et al.*, 2008]), TR163-22 (circles [*Lea et al.*, 2006]), and Site 1242 (diamonds: solid, $^{14}$C; open, $\delta^{18}$O tie points [*Benway et al.*, 2006]). See text for discussion of age models.

our record (I. Cacho et al., Tropics to high latitude teleconnections during past rapid climate changes: The seasonality paradox, submitted to *Quaternary Science Reviews*, 2008).

### 3.3. N Content and Stable Isotope Measurements

[10] Nitrogen isotope ratios ($\delta^{15}$N, ‰) and total nitrogen contents (TN, wt%) were determined on dried, ground bulk sediment. Samples from Site 1240 were measured on Carlo Erba 1500 series elemental analyzer equipped with a Costech zero-blank autosample coupled to a ThermoFinnigan Delta $Plus_{XL}$ isotope ratio mass spectrometer (IRMS) at Oregon State University (OSU) with additional analyses made on a Costech 4010 Elemental Analyzer (EA) with zero blank autosampler coupled to a Thermo Delta V IRMS at the University of Rhode Island (URI). All of the TR163-22 data was collected at the URI IRMS laboratory. An intercomparison between the URI and OSU laboratories was made using overlapping samples from Site 1240 to assure no systematic offsets between the data. The $\delta^{15}$N data from Site 1242 were generated separately at the University of Bordeaux using a Carlo Erba 2500 EA coupled to an Isoprime Micromass IRMS. The precision of the isotopic analyses based on replicates of standards and samples is better than ±0.3‰ for all labs. Precision on the TN analysis is ±0.01%. Nitrogen isotopic values are reported in delta ($\delta$) notation where: $\delta^{15}N = (((^{15}N/^{14}N_{sample}/^{15}N/^{14}N_{standard}) - 1) \times 1000$, and the standard is atmospheric $N_2$. Low resolution, ~30% of total sample set, organic carbon concentration measurements made on acidified samples from Sites 1240 and 1242 show no significant change in the carbon-to-nitrogen ratio of the buried organic matter and indicate that TN concentrations reflect the relative variation in organic carbon contents. A small positive intercept, ($\leq$0.075, not shown) in a crossplot of TN and $C_{org}$ at both sites indicates that some inorganic nitrogen is present in the sediments, likely as ammonium in clays [*Martinez and Robinson*, 2009]. It is insignificant relative to the organic N contributions and should not impact the N isotopes.

## 4. Results

### 4.1. Coherent Variation in Sedimentary Nitrogen Contents Across the ETP

[11] Weight percent TN records reveal a regionally coherent pattern of change in organic matter concentrations across the last ~40 ky (Figure 2). TN concentrations are moderate during the glacial between 40 and 20 ka, increasing to a maximum between 16 and 17 ka and then rapidly declining to overall lower values between 0 and 14 ka. In all three sites there is a small peak during the Holocene around 11–12 ka. Site 1242 has a less pronounced deglacial peak in TN as a result of higher overall TN during the LGM. However, it drops off in a similar fashion at the end of Termination 1. There are geographical differences in organic matter concentrations, with the higher overall concentrations at Sites 1240 and 1242. This pattern is predictable given that Site 1240 is located within the highly productive Equatorial cold tongue and Site 1242 is located on the continental margin while TR163-22 sits farther from the core of the cold tongue within the EEP. Each of these sites receives varying amounts of other biogenic sediments, such as opal and calcium carbonate, as well as vastly different amounts of lithogenic contributions between the margin and the EEP that likely serve to dilute TN to varying degrees.

### 4.2. Regional Variation in Bulk Sedimentary $\delta^{15}$N

[12] Changes in sedimentary $\delta^{15}$N in the two equatorial sites are generally similar during the last 40 ky, with lower $\delta^{15}$N, in the 4–5‰ range between 20 and 40 ka and a ~2‰ increase that begins around 20 ka (Figure 2). Both at 1240 and at TR163-22 $\delta^{15}$N achieves a maximum in the early Holocene, around 6–8 ka, but 1240 shows an earlier peak at 13–14 ka followed by a short depletion at 13–9 ka which is not identified in the TR163-22 record. After the initial increase, that starts around 20 ka at all three sites, the $\delta^{15}$N record at Site 1242 is distinct from the two equatorial

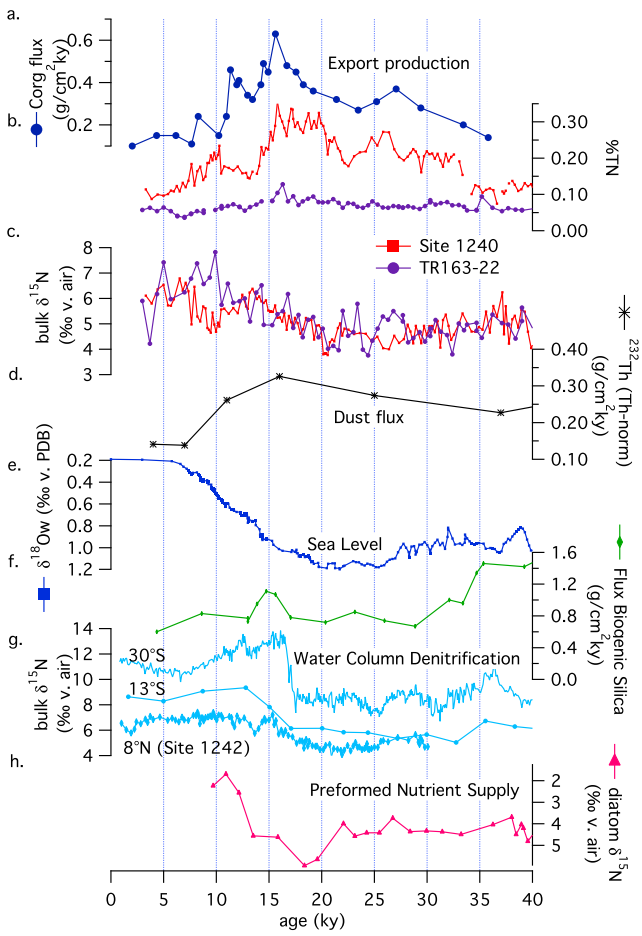


**Figure 3.** (a) Changes in export productivity ($C_{org}$ AR) in the EEP from ME00005A-24JC [*M. Kienast et al.*, 2006] do not correspond to variation in $\delta^{15}N$ at Site 1240 and TR163-22 in the EEP although (b) % total nitrogen (TN) shows good agreement with the AR record. (c) The variation in $\delta^{15}N$ at Site 1240 (red squares) and TR163-22 (purple circles) in the EEP. Fe driven changes in the relative demand for nitrate may be controlled by changes in detrital Fe inputs via the atmosphere or sea level related changes in erosion of Fe-bearing sediments, as illustrated by changes in (d) $^{230}$Th-normalized $^{232}$Th AR at ODP 849 [*Winckler et al.*, 2008] and (e) $\delta^{18}O_w$ [*Siddall et al.*, 2003; *Lambeck and Chappell*, 2001]. (f) Changes in silicate supply are approximated by a biogenic silica accumulation rate record from nearby TR163-19 [*S. S. Kienast et al.*, 2006]. Potential source driven changes in $\delta^{15}N$ may be due to (g) changes in water column denitrification in the ETP illustrated by sedimentary $\delta^{15}N$ records from Chile (GeoB7139-2, 30°S [*De Pol-Holz et al.*, 2007]), Peru (CD38-02, 13°S [*Ganeshram et al.*, 2000]), and the Central American margin (ODP Site 1242) [*Martinez and Robinson*, 2009] or, less proximally, (h) variation in the extent of nutrient consumption in the Subantarctic.

sites. At Site 1242, $\delta^{15}N$ peaks at 15 ka, drops briefly to a minimum centered at 14 ka, and then maintains relatively constant high values throughout the Holocene. In all cases, there is no coherent relation between the TN records and the bulk $\delta^{15}N$. All data are available at NOAA's WDS for Paleoclimatology web server: http://www.ncdc.noaa.gov/paleo/data.html.

## 5. Discussion

### 5.1. Reexamining $\delta^{15}N$ With Respect to Export Production in the EEP

[13] In the EEP records shown here, variation in sedimentary $\delta^{15}N$ is related to TN content in the same way that $\delta^{15}N$ and organic carbon ($C_{org}$) were related in the *Farrell et al.* [1995] comparison, they almost, but not quite, mirror one another. If we compare $\delta^{15}N$ to $^{230}$Th-normalized $C_{org}$ AR from core ME0005A-24JC, a site survey core raised from nominally the same location as Site 1240 [*M. Kienast et al.*, 2006], the difference in phasing is emphasized (Figures 3a–3c). There is general agreement between the weight percent $C_{org}$ and TN records at ME0005A-24JC and Site 1240, respectively, between 13 and 35 ka indicating that timing offsets due to age model differences are minor during the deglaciation (Figures 3a and 3b). There are more obvious differences during the Holocene. The consistency of the age models of these two cores is also supported by good agreement between UK37 records from each (Cacho et al., submitted manuscript, 2008). Since %$C_{org}$ is susceptible to dilution, we use the $^{230}$Th-normalized $C_{org}$ AR record as our primary indicator of export changes. $C_{org}$ AR begins to increase around 23ky, but the $\delta^{15}N$ rise does not begin until ~20ky. More importantly, $C_{org}$ AR peaks and then begins to decline at ~16ky while $\delta^{15}N$ continues its rise toward a peak at ~14ky at Site 1240 and a bit later at TR163-22. The good agreement between TN in the Site 1240 and TR163-22 and weight percent $C_{org}$ and $^{230}$Th-normalized $C_{org}$ AR in ME0005A-24JC suggests that there may have been a broadly regional peak in productivity during the deglaciation that extends to the margin if one includes Site 1242 in the comparison (Figures 3a and 3b). Again, the weight percent organic matter measurements are not ideal indictors of export productivity and additional $^{230}$Th-based measurements are needed for confirmation of this pattern. The N isotope records in the EEP suggest a regional change in $\delta^{15}N$ across the glacial interglacial transition; this change does not relate directly to export.

### 5.2. Controls on Nutrient Consumption

[14] Productivity changes need not be reflected in the sedimentary $\delta^{15}N$ record, since the relative consumption of nitrate depends not only on the demand for nutrients but also on the supply as *Farrell et al.* [1995] noted. For example, if supply and demand are relatively balanced so that they change in tandem, the $\delta^{15}N$ of nitrate, and ultimately sedimentary $\delta^{15}N$ will not change in step with export productivity. Since the uptake of nitrate in the Equatorial Pacific is ultimately controlled by the availability of iron [*Chai et al.*, 1996; *Fitzwater et al.*, 1996; *Martin et al.*, 1991] changes in the degree of nitrate consumption require that the surface waters witness variations in the iron-to-nitrate ratio (Fe:$NO_3^-$) and not just the net supply of nutrients.

[15] The deglacial increase in $\delta^{15}N$ might indicate an increase in atmospheric Fe deposition or in the Fe content of the EUC. However, $^{230}$Th-normalized $^{232}$Th records of

detrital AR from the Equatorial Pacific indicate that Fe deposition was higher during the LGM, likely due to the increased dustiness of the glacial atmosphere (Figure 3d) [*McGee et al.*, 2007; *Pichat et al.*, 2004; *Winckler et al.*, 2008]. Assuming nitrate flux was constant, eolian Fe fertilization would drive an increase in nutrient consumption during the last ice age, which is not consistent with our data. Alternatively, the Fe:$NO_3^-$ of the EUC waters may have increased. Fe in the EUC is acquired through remineralization of organic matter and lithogenic and hydrothermal inputs along the water mass' flow path.

[16] It has been argued that the Fe content of the EUC is set at its origin in the western Pacific when the various coastal currents that feed into EUC are in contact with northern coast of Papua New Guinea [*Sholkovitz et al.*, 1999; *Wells et al.*, 1999]. This tectonically active, convergent island arc region has experienced variable amounts of volcanic, erosional, and hydrothermal activity over the Neogene. *Wells et al.* [1999] demonstrated that small changes in erosional or hydrothermal iron inputs have the potential to stimulate productivity all the way across the Pacific in the EEP. *Altabet* [2001] extended this idea to the $\delta^{15}$N record and suggested that glacial/interglacial sea level changes affect the Fe:$NO_3^-$ of EUC source waters such that Fe inputs are larger during interglacial episodes. This is counter to idea that lithogenic inputs are greater during sea level lowstands and requires a source of Fe during periods of higher sea level. If this Fe was the product of enhanced erosional inputs, there is no evidence for an increase in Fe inputs during the deglacial in the $^{232}$Th records of detrital inputs nor in trace element geochemical records from across the equator [*McGee et al.*, 2007; *Pichat et al.*, 2004; *Winckler et al.*, 2008; *Ziegler et al.*, 2008]. Yet, if we compare the initiation of the deglacial $\delta^{15}$N change at both Site 1240 and TR163-22 to the decrease in benthic $\delta^{18}O_w$ from a composite record that describes the deglacial eustatic sea level rise [*Lambeck and Chappell*, 2001; *Siddall et al.*, 2003], the initial shifts are nearly coincident (Figure 3e). Although we cannot completely rule out the possibility of Fe:$NO_3^-$ related changes in the EUC as a function of sea level, the available geochemical data indicate that this is not the primary control on the $\delta^{15}$N record.

[17] Changes in Fe:$NO_3^-$ could also be a function of changes in preformed nitrate content of SAMW, the ultimate source of EUC [*Loubere et al.*, 2004, 2007; *Robinson et al.*, 2007; *Spero and Lea*, 2002]. Entrainment of relatively nitrate-rich Subantarctic surface waters into SAMW would increase nitrate concentrations in the EUC. However, diatom $\delta^{15}$N records from the Antarctic and Subantarctic Pacific Zones of the Southern Ocean indicate that nitrate supply was likely lower during the last ice age and it increased upon deglaciation (Figure 3h) [*Robinson et al.*, 2004, 2005]. Much the same pattern of change, with lower glacial preformed nutrients in the EUC, and an increase upon deglaciation, are also inferred from a changes in planktonic foraminiferal $\delta^{13}$C in the EEP [*Loubere*, 2000; *Loubere et al.*, 2007; *Pena et al.*, 2008; *Spero and Lea*, 2002]. And, although this pattern fits well with the pattern of export, it does not explain the observed variation in sedimentary $\delta^{15}$N.

[18] Silicate has been hypothesized to colimit nitrate uptake in the EEP [*Dugdale and Wilkerson*, 2001]. Changes in the supply of silicate may be inferred through comparison of the AR of biogenic silica on the seafloor with changes in $\delta^{30}$Si [*S. S. Kienast et al.*, 2006; *Pichevin et al.*, 2009]. A broad regional peak in opal AR occurs around 50 ka and then steadily declines toward low values in the LGM followed by an increase in opal ARs during the deglaciation (Figure 3f) [*S. S. Kienast et al.*, 2006; *Pichevin et al.*, 2009]. The increase in opal AR is accompanied by an increase in the $\delta^{30}$Si, indicating an increase in the relative utilization of silicic acid during the deglaciation [*Pichevin et al.*, 2009]. Fe fertilization causes a decrease in the uptake ratio of silicic acid to nitrate by diatoms [*Hutchins and Bruland*, 1998; *Takeda*, 1998] and results in more weakly silicified diatoms. The observed changes in opal AR and $\delta^{30}$Si in the EEP likely reflect the transition from glacial, eolian Fe-replete conditions, when silicic acid demand by diatoms would be low as would opal burial rates, to interglacial times. During the interglacial, dust delivery was significantly lower, and both silicic acid demand and opal burial would be elevated [*Pichevin et al.*, 2009]. The expected result of an Fe mediated shift in silicic acid uptake in the nitrogen isotope record is a decrease in $\delta^{15}$N upon deglaciation, due to the increasing Si:N of uptake by diatoms. However, the $\delta^{30}$Si record does not bear a coherent relationship to the observed changes in $\delta^{15}$N.

### 5.3. Changes in Isotopic Composition of Source Nitrate

[19] The spatial distribution of surface sedimentary $\delta^{15}$N reflects the isotopic composition of the source nitrate and the degree of nitrate consumption in the surface ocean of the EEP (Figure 1) [*Farrell et al.*, 1995]. Since the observed temporal variation in $\delta^{15}$N does not vary coherently with export productivity or with potential variations in the Fe:$NO_3^-$ of the surface waters, the assumption that the $\delta^{15}$N of the upwelled nitrate in the EEP did not change on glacial/interglacial timescales [*Farrell et al.*, 1995] must be explored. Glacial-interglacial scale changes in the $\delta^{15}$N of nitrate are thought to have occurred at both the ultimate (SAMW) and the proximal (Peru) sources of nitrate to the EEP. The $\delta^{15}$N of nitrate in SAMW is a mixture of Subantarctic surface waters and subtropical thermocline waters [*Sigman et al.*, 2000]. The concentration of nitrate in Subantarctic surface waters entering SAMW at present is $\sim$18 $\mu$M with a $\delta^{15}$N slightly greater than 5‰. It is likely diluted and somewhat isotopically altered in the subsurface where it mixes with subtropical thermocline water. If we assume that SAMW has a concentration of $\sim$15 $\mu$M, then its starting concentration is 30–50% of the total subsurface $NO_3^-$ offshore Peru. The additional >50% of the nitrate offshore Peru comes from the remineralization of organic matter along SAMW's flow path. Remineralized nitrate has an isotopic composition that is approximately equal to $\delta^{15}$N of the sinking organic nitrogen. Outside of the HNLC regions, nitrate is completely consumed in the surface ocean so that the $\delta^{15}$N of sinking organic material is equal to that of the subsurface nitrate [*Sigman et al.*, 2000] and, at present, we have no good evidence for or against a change

in deep ocean $\delta^{15}$N-nitrate on glacial/interglacial timescales. Our best first-order approximation of a shift in the $\delta^{15}$N of preformed nitrate in EUC is based on the diatom $\delta^{15}$N records from the Southern Ocean [*Robinson et al.*, 2005]. They indicate that any change in the EUC would be toward higher $\delta^{15}$N during the LGM and a decrease upon deglaciation, opposite of the observations (Figure 3h) [*Robinson et al.*, 2005]. Another explanation is needed.

[20] Regional changes in sedimentary $\delta^{15}$N that reflect variation in the extent of denitrification within the large region of water column suboxia in the ETP are well documented for the time interval 0–40 ka [*De Pol-Holz et al.*, 2006, 2009; *Ganeshram et al.*, 1995, 2000; *Hendy et al.*, 2004; *Robinson et al.*, 2007]. In the modern, subsurface $\delta^{15}$N-nitrate in the suboxic waters offshore Peru has been measured as high as 30‰ as a result of the high isotope effect of denitrification [*Liu and Kaplan*, 1989]. Upwelling of the $^{15}$N enriched nitrate from within the suboxic zone results in the incorporation of this signal in the sedimentary record. Moreover, downcore records exhibiting the changes in $\delta^{15}$N associated with denitrification are not restricted to regions of active water column denitrification. Advection in the subsurface carries the isotopic signal as far as the Subantarctic Front in the SE Pacific [*Martinez et al.*, 2006], Oregon and British Columbia in the NE Pacific [*Kienast et al.*, 2002], the subarctic North Pacific [*Galbraith et al.*, 2008], and the Okinawa Trough [*Kao et al.*, 2008] and the Indonesian Throughflow [*Kienast et al.*, 2008] in the western Pacific. The pattern in margin sedimentary $\delta^{15}$N records, with glacial periods bearing lower $\delta^{15}$N relative to interglacial periods, fits with what is observed in the EEP records (Figures 3g).

[21] A comparison of the *Farrell et al.* [1995] surface sediment data to annual surface nitrate concentrations indicates that the EEP is dominated by a single source of nitrate (Figures 1a, 1c, and 1d). Nitrate concentrations peak around 5°S and decrease to the north and south. The $\delta^{15}$N of surface sediment increases with decreasing nitrate concentrations away from the nitrate maximum. There is no indication of significant input of nitrate at the Equator nor is there a change in the sedimentary $\delta^{15}$N north of the Equator indicative of a secondary source of nitrate. Sedimentary $\delta^{15}$N is linearly related to ln [$NO_3^-$] in the region north of 3°S, suggesting that the uptake and assimilation of upwelled nitrate entrained in the dominant surface circulation is regulating the spatial distribution of $\delta^{15}$N. The slope here is an approximation of the isotope effect of nitrate assimilation and the value, $\varepsilon = -2$‰, is essentially the same as previous estimates from the Equatorial Pacific [*Altabet*, 2001; *Altabet and Francois*, 1994]. Overall, the trend is cleaner in the longitude band between 90°W and the coast of the Americas (Figure 1d, solid squares). However, the same pattern is apparent, with an increase in $\delta^{15}$N with decreasing [$NO_3^-$] north of the equator further west toward the central Pacific although with more associated scatter. South of 3°S, there is no clear relationship between the ln [$NO_3^-$] and $\delta^{15}$N in surface sediment. Surface sediments bear a range of $\delta^{15}$N that is nearly as large as for the entire 13° latitude covered to the north. The enrichment in $\delta^{15}$N south of the equator is due to significant upwelling of nitrate bearing the high $\delta^{15}$N signature of denitrification along the margin. Despite this clear difference between the sediment located to the north and south of the equator, both the linear trend and the band of scatter extend out from approximately the same starting [$NO_3^-$] and $\delta^{15}$N. The $\delta^{15}$N, 6‰, is slightly above the global oceanic mean (5‰), and similar to modern Equatorial subsurface waters at 90°W (R. S. Robinson and D. M. Sigman, unpublished data, 2004).

[22] This observation suggests that an isotopically uniform nitrate pool that is enriched relative to the oceanic mean underlies the EEP and the northern edge of the Peru upwelling. The pronounced enrichment in samples south of the equator is likely due to active exchange between the subsurface nitrate underlying the EEP and the denitrified water offshore Peru. The isotopic composition of subsurface nitrate offshore Peru between 8 and 4°S lies between 6 to 8.5‰. Assuming that the EUC delivers nitrate with an isotopic composition of 5‰ and a $\delta^{15}$N of the subsurface $NO_3^-$ pool on the equator equal to 6‰ [*Farrell et al.*, 1995; Robinson and Sigman, unpublished data, 2004], we estimate a minimum of 30% of the total nitrate pool must come from exchange with or advection from the Peru margin OMZ. Either of the physical explanations for the asymmetrical nitrate maximum and temperature minimum in the EEP can drive this exchange. If nitrate were upwelling off of Peru and advected westward at the surface, then nitrate may be progressively consumed along its path. There is no evidence for a zonal increase in $\delta^{15}$N comparable to what is seen with latitude, indicating that surface advection is not likely. If significant, one might expect $\delta^{15}$N at TR163-22 to be higher than at Site 1240.

[23] In the subsurface, two low $O_2$ tongues extend across the Pacific from the oxygen minimum zones (OMZ) in the ETP (Figure 1). The high $\delta^{15}$N signature of the OMZs is likely transported westward within these water masses. Furthermore, since the Southern tongue underlies the surface expression of the nitrate tongue, we interpret it to be the source of the $^{15}$N-enriched nitrate to the EEP. It follows then that changes in the $\delta^{15}$N of nitrate on the margin should impact the $\delta^{15}$N records in the EEP.

[24] Comparison of multiple records of water column denitrification from the margins of the Americas, including Site 1242, introduced here, reveals gross similarities between all of the records and the EEP records (Figures 3c and 3g) however there are some clear differences. In particular, the timing of the deglacial increase in $\delta^{15}$N occurs quite early and very rapidly in the Chile margin record (GeoB7139-2) [*De Pol-Holz et al.*, 2007] relative to a lower resolution record from offshore Peru at 13°S (CD38-02) [*Ganeshram et al.*, 2000]. Site 1242 sits right on the edge of region of modern water column denitrification and shows an increase in $\delta^{15}$N that begins at about the same time as the rise off Peru and in the EEP sites, but achieves a peak sooner [*Martinez and Robinson*, 2009; *Ganeshram et al.*, 2000].

[25] Taking a longer view, a smoothed sedimentary $\delta^{15}$N at Site 1240, with a resolution of ~3ky, is very similar to the denitrification record from off Peru from CD38-02 (13°S), with a clear minimum at 70ky and maxima at 14 and 130ky (Figure 4) [*Ganeshram et al.*, 2000]. The amplitudes of

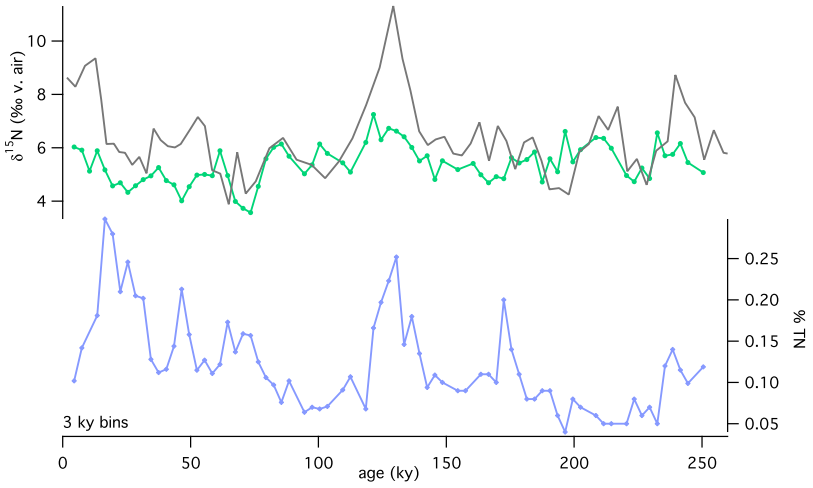


**Figure 4.** Smoothed (3 ky) $\delta^{15}$N and %TN data from ODP Site 1240 for the last 250 ky. Sedimentary $\delta^{15}$N is plotted on the same axis with a sedimentary $\delta^{15}$N record from the Peru margin (13°S) (solid gray line) for comparison to denitrification changes over multiple glacial cycles [*Ganeshram et al.*, 2000].

change are also variable between various records of denitrification. For example at Termination 1, the shift is 4‰ offshore Chile, ~3‰ offshore Peru, and 2‰ in the Panama Basin and ~2‰ in the EEP. Interestingly, the sites with the most rapid and highest amplitude changes are not regions of intense local water column denitrification but rather remote localities that receive nitrate with the isotopic signature of denitrification via the poleward undercurrents [e.g., *De Pol-Holz et al.*, 2007; *Emmer and Thunell*, 2000; *Hendy et al.*, 2004; *Kienast et al.*, 2002; *Pride et al.*, 1999; *Robinson et al.*, 2007]. The higher amplitudes likely result from the advection and progressive consumption of the nitrate pool as it is transported through the region of water column denitrification.

[26] The similarity in the source signatures throughout the EEP, as inferred from the surface sediment data set and the general coherence in the paleorecords, is analogous to the situation on the margins. The signature of denitrification is carried along the margins by the poleward undercurrents and delivered to the surface for uptake and assimilation via upwelling. In the EEP, the low oxygen tongue coming offshore Peru is apparently a significant source of nitrate to the Equatorial upwelling system. The long distance advection of these low oxygen, high $\delta^{15}$N nitrate water masses is likely the origin of the signal in the far Western Pacific as well [*Kao et al.*, 2008]. The fit is not perfect between the EEP and the margin record or even between the various marginal records because each locality witnesses both the large scale changes in denitrification as well as local influences including but not limited to variations in the amount or $\delta^{15}$N of source nitrate, changes in relative utilization, and possibly local nitrogen fixation and/or diagenesis. Given the excess nitrate in the EEP and the relatively high organic contents of the sediments, changes in the relative utilization of nitrate are likely the largest source of variability and what we focus on here.

### 5.4. Interpreting Regionally Overprinted $\delta^{15}$N Records

[27] If we accept that the EEP $\delta^{15}$N record is an amalgam of processes, the pertinent questions become 1). Which is more important in controlling the sedimentary $\delta^{15}$N record in the EEP, variations in denitrification or changes in the relative utilization of nitrate? And 2.) Can useful information related to nitrate consumption be extracted from this overprinted record? In order to isolate the changes in the isotopic composition of nitrate coming from Peru from those due to variation in the consumption of nitrate in the EEP proper, we need an accurate estimate of the source $\delta^{15}$N. Ideally, we would use a high resolution stacked record of $\delta^{15}$N offshore Peru, or even a single record from a site underlying the northern edge of the region of water column denitrification. But neither exist. The longer record from 13°S, CD38-08, is too low resolution for our purposes. Moreover, $NO_3^-$ is not completely consumed in surface waters above the northern edge of the denitrification region and age control is difficult, making generating such a record of denitrification changes offshore Peru difficult to near impossible [*De Pol-Holz et al.*, 2009].

[28] In a preliminary attempt to extract the denitrification signal, we will subtract the $\delta^{15}$N record from Site 1242 and core GeoB7139-2 from the two EEP records over the last 30 ky. Site 1242 lies on the eastern edge of the Panama Basin and the surface waters overlying both 1242, the Peru margin, and the EEP are similarly depleted in radiocarbon, indicating origin in the EUC and ultimately in SAMW [*Toggweiler et al.*, 1991]. Any variation in the $\delta^{15}$N of nitrate in SAMW should be similar at all three sites used. Nitrate is completely utilized at the sea surface and oxygen is nearly gone in the subsurface overlying Site 1242, with average $[O_2]$ of 5–6 $\mu$M [*Garcia et al.*, 2006a]. 6–10 $\mu$M is the apparent threshold for active denitrification. The sedimentary $\delta^{15}$N record at 1242 reflects local, likely seasonal, changes in the extent of water column denitrification. The

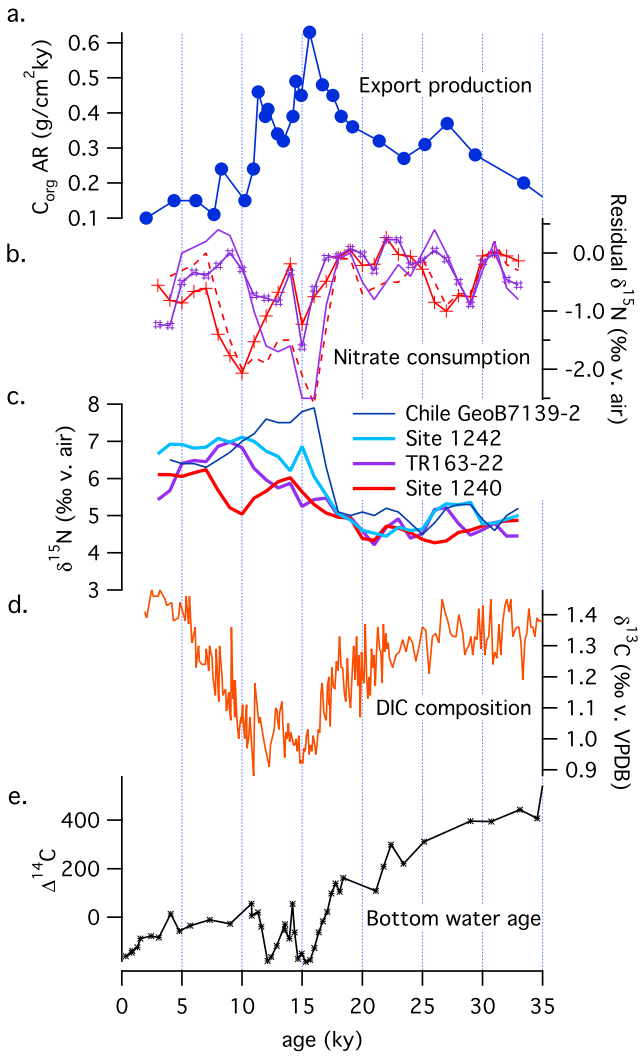


**Figure 5.** (a) $C_{org}$ AR at ME0005A-24JC [*M. Kienast et al.*, 2006]; (b) residual $\delta^{15}$N (1240 (line with crosses) or TR163-22 (line with pound signs) $\delta^{15}$N minus 1242 $\delta^{15}$N and 1240 (dashed line) or TR163-22 (solid line) minus Chile GeoB7139-2) [*De Pol-Holz et al.*, 2007]; (c) the smoothed and resampled (1ky) 1240, TR163-22, Chile GeoB7139-2, and 1242 sedimentary $\delta^{15}$N records used in calculating the residual $\delta^{15}$N records; (d) planktonic foraminiferal $\delta^{13}$C (*N. dutertrei*) from Site 1240 [*Pena et al.*, 2008]; and (e) radiocarbon composition of benthic forams from off Baja California in the NE Pacific [*Marchitto et al.*, 2007]. The extraction of the overprinting denitrification signal represented by changes in $\delta^{15}$N at Site1242 and Chile GeoB7139-2 from the EEP record gives a good first approximation of nutrient supply and demand changes in the EEP. Together, the residual $\delta^{15}$N and $\delta^{13}$C records indicate nutrient supply to the EEP increased significantly during the deglaciation.

temporal pattern at 1242 is quite similar to southern hemisphere records of water column denitrification from the Peru and Chile margins. This is particularly clear during the early increase in $\delta^{15}$N, initiating at ~17.5 ky to a peak around 15–16 ky followed by a short dip centered around 14 ky, during the Antarctic Cold Reversal. Site 1242 differs in its amplitude of change, which is smaller. In this respect, variation at Site 1242 scales better with the changes observed at Site 1240 and TR163-22.

[29] The small amplitude of change is likely because Site 1242 sits at the leading edge of the region of modern water column denitrification. The subsurface water that bathes the core site and is upwelled to the surface is delivered from a region that does not witness significant active water column denitrification prior to its arrival over Site 1242. As a result, there is likely little accumulation, or progressive enrichment, of the isotopic signal during transport through the suboxic zone to amplify the variation in the $\delta^{15}$N. In sum, the $\delta^{15}$N record from Site 1242 represents a conservative estimate of changes in denitrification that appear to be representative of the larger region as a whole [*De Pol-Holz et al.*, 2007; *Ganeshram et al.*, 2000; *Hendy and Pedersen*, 2006; *Robinson et al.*, 2007]. At the same time, it excludes potential complications associated with local utilization signals [*De Pol-Holz et al.*, 2009] or the accumulation of $^{15}$N enriched nitrate that appears to occur with transport of the subsurface nitrate pool along the margins. For comparison, we subtract the previously published bulk $\delta^{15}$N record from Chilean core GeoB7139-2, located at 30°S [*De Pol-Holz et al.*, 2007]. This record has significantly greater absolute values and shows a higher amplitude of change than Site 1242. However, because it sits downstream of the core of the Peru OMZ, it also records a regionally integrated signal.

[30] We removed the denitrification signal by subtracting the Site 1242 and GeoB7139-2 $\delta^{15}$N records from that of Site 1240 and TR163-22. A similar procedure was used by *Galbraith et al.* [2008] to wash the denitrification signal from a record located in the subarctic Pacific. First the four records were smoothed to a 1 ky sampling interval to eliminate potential bias due to age model errors and sampled on a common age scale. We assumed that the record at 1242 reflected the $\delta^{15}$N of the regional subsurface nitrate pool without any attenuation of the signal. This assumption is based on our interpretation of the *Farrell et al.* [1995] surface sediment data when compared to surface ocean [$NO_3^-$] and the fact that the $\delta^{15}$N on the northern Peru margin at the edge of the region of denitrification is equivalent to what we have measured in the modern water column at 90°W (Robinson and Sigman, unpublished data, 2004). For GeoB7139-2, we scaled the record by multiplying the $\delta^{15}$N by a factor of 0.6. This brought the core top values down toward the regional $\delta^{15}$N in the EEP in an attempt to eliminate some of the effect of being so far downstream within the OMZ. Once removed, the variation in the residual $\delta^{15}$N at both EEP sites should reflect changes in utilization of nitrate. The residual $\delta^{15}$N has a propagated error of 0.42‰.

[31] The derived residual $\delta^{15}$N records show the highest $\delta^{15}$N during the LGM, decreasing to a low around 15–16 ka followed by short increase and then a second, smaller minimum that is centered around 12 ka at TR163-22 and 10 ka at Site 1240 (Figure 5). The residuals derived from substracting the Costa Rica margin record (1242) and the

Chile (GeoB7139-2) record, are qualitatively similar. The amplitudes are different, due to the large amplitude changes in the Chile record. Most importantly for this discussion, the distinct minimum at 15–16 ka, is apparent into both estimates of residual $\delta^{15}N$, and suggests that the most significant regional changes in $\delta^{15}N$ are recorded with only small offsets in timing between Costa Rica and Chile. However, the relatively large differences in the later Holocene emphasize the fact that there are both regional and local influences on $\delta^{15}N$ that add uncertainty to this exercise.

[32] The origin of the differences between the TR163-22 and the Site 1240 residuals (and the difference between the two records around 10 ka) is likely related to regional heterogeneity in upwelling and productivity, perhaps associated with the presence of the Galapagos Islands between the two sites or their proximity to the North Equatorial Front and the intertropical convergence zone. Interpreting the derived residuals as records of local nutrient consumption, they indicate that the degree of consumption was greatest during the LGM when, according to the $C_{org}$ record, productivity was higher than during the late Holocene but not at its maximum for the interval. The LGM is also the period when the dust records indicate that Fe:$NO_3^-$ was highest (Figure 3g). This situation changed notably after 19 ka. The residual $\delta^{15}N$ indicates an increase in nitrate availability (weaker nitrate consumption) (Figure 5b) at the same time that $C_{org}$ accumulation (and concentrations) increased (Figure 5a) [*M. Kienast et al.*, 2006]. This change in nutrient availability is further supported by a $\delta^{13}C$ record from the planktonic foraminifera *Neogloboquadrina dutertrei* from Site 1240 (Figure 5d). The significant decrease in $\delta^{13}C$ after 19 ka and across the termination is interpreted to indicate enhanced arrival of nutrient rich waters into the EEP through the EUC [*Pena et al.*, 2008] (Figure 5). The deglaciation was a highly productive episode and nutrient supply must have been much greater than demand. Since the deglaciation was a time of significant decreases in dust flux (Figure 3g), the reduction in nutrient consumption is likely due, in part, to enhanced Fe limitation.

[33] However, changes in Fe supply inferred from the dust records cannot adequately explain the observed pattern of changes in nutrient consumption. The two minima in nutrient consumption inferred from the residual $\delta^{15}N$ record are associated with significantly different detrital fluxes. The foraminifera $\delta^{13}C$ minima observed during the deglaciation at nearby site TR163-19 [*Spero and Lea*, 2002], and Site 1240 (Figure 4) [*Pena et al.*, 2008], are interpreted as the result of a resumption of deep overturning in the Southern Ocean and the reemergence of nutrient-rich water that was isolated in the deep ocean during the glacial period. Parallel increases in the EUC salinity signal during these intervals suggest that a stronger EUC flux enhanced upwelling conditions in the EEP [*Pena et al.*, 2008]. In line with this thinking, *Marchitto et al.* [2007] measured significant decreases in benthic foraminiferal $\Delta^{14}C$, greater than could be explained by changes in atmospheric $^{14}C$ production, from intermediate depths, during Heinrich event 1 and the Younger Dryas [*Marchitto et al.*, 2007] off of Baja California. The minima likely resulted from the influx of old, nutrient and $CO_2$ rich bottom waters during the deglaciation [*Marchitto et al.*, 2007]. These minima are approximately synchronous with peaks in export production and low relative nutrient utilization inferred from the residual $\delta^{15}N$ (TR163-22 in particular) and $\delta^{13}C$ records (Figure 4). The resumption of overturning and the influx of nutrients into the low latitude thermocline during the deglaciation likely lead to the significant regional increase in export productivity and to the observed shift in nutrient supply and demand dynamics in the EEP. The ~250 ky $\delta^{15}N$ and $\delta^{13}C$ records from Site 1240 indicate that this infusion of nutrient-rich waters to intermediate depths was a transient feature of at least the last three deglaciations (Figure 4) [*Pena et al.*, 2008].

[34] An increase in the rate of nutrient supply, rather than the nutrient content of the upwelled water, could also lead to a reduction in the consumption of nutrients at times of high export as observed here. Changes in the upwelling rate were inferred by *M. Kienast et al.* [2006] to explain the coincident increase in export and decrease in alkenone-based sea surface temperature at ~15 ka (approximately Heinrich event 1 (H1)) in the EEP. Cacho et al. (submitted manuscript, 2008) propose that precession-forced increases in seasonality in the equatorial Pacific led to cooling and more "La-Niña-like" conditions during the deglaciation [*Pena et al.*, 2008] that were reinforced by slowdowns in Atlantic meridional overturning circulation associated with the Younger Dryas and H1. However, if nitrate uptake in the EEP is truly Fe limited, the observed change in nitrate consumption indicates that the Fe:$NO_3^-$ in the surface water must be affected by the rate of upwelling. So, if upwelling rate changes are driving the observed peaks in export coincident with decreased utilization, then delivery of atmospherically derived Fe (rather than upwelled EUC derived Fe) is critical to the ecosystem in the EEP. The late Holocene witnessed a more moderate degree of nutrient consumption and the lowest export productivity of the entire record. The residual $\delta^{15}N$ is lower in the Holocene interval than during the mean glacial situation. This general difference fits with detrital flux records which show overall that Fe supply was relatively low during the Holocene [*McGee et al.*, 2007; *Pichat et al.*, 2004; *Winckler et al.*, 2008] and emphasize the potential role for atmospheric Fe. In addition, Fe delivery has secondary impact on the consumption of $NO_3^-$ through its influence on the Si:N uptake by diatoms. The reconstructed changes in nitrate utilization fit in a general sense with the observed changes in $\delta^{30}Si$, where lower $\delta^{30}Si$ values occur when the residual $\delta^{15}N$ is high during the glacial and both shift, in an opposite sense, upon deglaciation [*Pichevin et al.*, 2009]. The absolute minimum in $\delta^{15}N$, observed around 15ky, is not apparent in the $\delta^{30}Si$ record and requires an increase in the supply of nutrient N that exceeds demand and not just a glacial-interglacial style shift in Fe inputs.

[35] The extraction of the denitrification signal from the EEP record allows for the examination of nutrient supply changes to the region and may also provide an explanation for the origin of the overprinting signal: the abrupt increase in the rates of denitrification downstream from the EEP. The enhanced supply of nutrients and peaks in export occur at approximately the same time as the regional peak in

denitrification in the early Holocene. The maximum in export indicates that subsurface oxygen demand must also have been at a maximum in the EEP. Drawdown under the equatorial upwelling system likely reduced the supply of oxygen to the marginal OMZs, working to increase the extent of suboxia and rates of water column denitrification [*Martinez and Robinson*, 2009].

## 6. Summary

[36] Two new records of nitrogen content and sedimentary $\delta^{15}N$ from the EEP reveal regionally coherent productivity and $\delta^{15}N$ records. However, there is no clear relationship between the two proxies. Variation in bulk $\delta^{15}N$ cannot be explained by changes in export productivity or Fe availability, the supposed primary control on the uptake and assimilation of nitrate in the EEP. The spatial distribution of surface sedimentary $\delta^{15}N$ and the downcore variability suggest that the $\delta^{15}N$ of the source nitrate is impacted by water column denitrification offshore Peru. Widespread regional overprinting by the advection of water masses carrying the isotopic signature of denitrification significantly masks the local uptake and assimilation signal in the nitrate replete EEP. However, obvious deviations in the pattern of $\delta^{15}N$ change and coherent spatial variation with respect to surface nitrate concentrations suggest that nutrient utilization is also recorded by the sedimentary $\delta^{15}N$. Subtraction of an inferred regional denitrification signal results in a residual $\delta^{15}N$ record for the EEP that varies coherently with available records of export productivity, surface nutrient content, and, to some degree, aeolian Fe. Nitrate consumption was highest during the glacial maximum when $Fe:NO_3^-$ was elevated due to atmospheric dust inputs and lowest during the deglacial peaks in export production. Reduced consumption during times of high export suggests that nutrient supply was at an absolute maximum during the deglaciation. The times of elevated supply appear to correspond to intervals of enhanced delivery of old, nutrient-rich water from the abyss to intermediate depths that are thought to be related to the release of $CO_2$ from the oceans during the deglaciation. The nutrient utilization data indicate that the EEP specifically would have been a larger than normal source of $CO_2$ to the atmosphere at this time. The resulting increase in export productivity would in turn have led to increase subsurface oxygen demand, potentially working to enhance suboxia and water column denitrification downstream in the OMZs. In sum, the EEP is both sensitive to and potentially regulating significant global biogeochemical processes that relate to large-scale changes in deep-ocean overturning, nitrate removal, and atmospheric $CO_2$ cycles.

[37] **Acknowledgments.** Thanks to M. Kienast, A. Mix, and R. Toggweiler for helpful discussions and two anonymous reviews that greatly improved this manuscript. Samples were provided by S. Carey from the University of Rhode Island's Rock and Core Facility and by ODP. Support for this work came from USSSP and the University of Rhode Island to R.S.R.

## References

Altabet, M. A. (2001), Nitrogen isotopic evidence for micronutrient control of fractional $NO_3^-$ utilization in the equatorial Pacific, *Limnol. Oceanogr.*, *46*, 368–380.

Altabet, M. A., and R. Francois (1994), Sedimentary nitrogen isotopic ratio as a recorder for surface ocean nitrate utilization, *Global Biogeochem. Cycles*, *8*(1), 103–116, doi:10.1029/93GB03396.

Altabet, M. A., et al. (1995), Climate-related variations in denitrification in the Arabian Sea from sediment $^{15}N/^{14}N$ ratios, *Nature*, *373*, 506–509, doi:10.1038/373506a0.

Altabet, M. A., et al. (2002), The effect of millennial-scale changes in Arabian Sea denitrification on atmospheric $CO_2$, *Nature*, *415*, 159–162, doi:10.1038/415159a.

Benway, H. M., A. C. Mix, B. A. Haley, and G. P. Klinkhammer (2006), Eastern Pacific Warm Pool paleosalinity and climate variability: 0–30 kyr, *Paleoceanography*, *21*, PA3008, doi:10.1029/2005PA001208.

Chai, F., et al. (1996), Origin and maintenance of a high nitrate condition in the equatorial Pacific, *Deep Sea Res., Part II*, *43*, 1031–1064, doi:10.1016/0967-0645(96)00029-X.

De Pol-Holz, R., O. Ulloa, L. Dezileau, J. Kaiser, F. Lamy, and D. Hebbeln (2006), Melting of the Patagonian Ice Sheet and deglacial perturbations of the nitrogen cycle in the eastern South Pacific, *Geophys. Res. Lett.*, *33*, L04704, doi:10.1029/2005GL024477.

De Pol-Holz, R., O. Ulloa, F. Lamy, L. Dezileau, P. Sabatier, and D. Hebbeln (2007), Late Quaternary variability of sedimentary nitrogen isotopes in the eastern South Pacific Ocean, *Paleoceanography*, *22*, PA2207, doi:10.1029/2006PA001308.

De Pol-Holz, R., et al. (2009), Controls on sedimentary nitrogen isotopes along the Chile margin, *Deep Sea Res., Part II*, *56*, 1042–1054, doi:10.1016/j.dsr2.2008.09.014.

Dugdale, R. C., and F. P. Wilkerson (2001), Sources and fates of silicon in the ocean: The role of diatoms in the climate and glacial cycles, *Sci. Mar.*, *65*, suppl. 2, 141–152, doi:10.3989/scimar.2001.65s2141.

Emmer, E., and R. C. Thunell (2000), Nitrogen isotope variations in Santa Barbara Basin sediments: Implications for denitrification in the eastern tropical North Pacific during the last 50,000 years, *Paleoceanography*, *15*, 377–387, doi:10.1029/1999PA000417.

Farrell, J. W., T. F. Pedersen, S. E. Calvert, and B. Nielsen (1995), Glacial-interglacial changes in nutrient utilization in the equatorial Pacific Ocean, *Nature*, *377*, 514–516, doi:10.1038/377514a0.

Fiedler, P. C., and L. D. Talley (2006), Hydrography of the eastern tropical Pacific: A review, *Prog. Oceanogr.*, *69*, 143–180, doi:10.1016/j.pocean.2006.03.008.

Fitzwater, S. E., K. H. Coale, R. M. Gordon, K. S. Johnson, and M. E. Ondrusek (1996), Iron deficiency and phytoplankton growth in the equatorial Pacific, *Deep Sea Res., Part II*, *43*, 995–1015, doi:10.1016/0967-0645(96)00033-1.

Galbraith, E. D., M. Kienast, S. L. Jaccard, T. F. Pedersen, B. G. Brunelle, D. M. Sigman, and T. Kiefer (2008), Consistent relationship between global climate and surface nitrate utilization in the western subarctic Pacific throughout the last 500 ka, *Paleoceanography*, *23*, PA2212, doi:10.1029/2007PA001518.

Ganeshram, R. S., et al. (1995), Large changes in oceanic nutrient inventories from glacial to interglacial periods, *Nature*, *376*, 755–757, doi:10.1038/376755a0.

Ganeshram, R. S., T. F. Pedersen, S. E. Calvert, G. W. McNeill, and M. R. Fontugne (2000), Glacial-interglacial variability in denitrification in the world's oceans: Causes and consequences, *Paleoceanography*, *15*(4), 361–376, doi:10.1029/1999PA000422.

Garcia, H. E., R. A. Locarnini, T. P. Boyer, and J. I. Antonov (2006a), *World Ocean Atlas 2005*, vol. 3, *Dissolved Oxygen, Apparent Oxygen Utilization, and Oxygen Saturation, NOAA Atlas NESDIS*, vol. 63, edited by S. Levitus, 342 pp., NOAA, Silver Spring, Md.

Garcia, H. E., R. A. Locarnini, T. P. Boyer, and J. I. Antonov (2006b), *World Ocean Atlas 2005*, vol. 4, *Nutrients (Phosphate, Nitrate, and Silicate), NOAA Atlas NESDIS*, vol. 64, edited by S. Levitus, 396 pp., NOAA, Silver Spring, Md.

Hendy, I. L., and T. F. Pedersen (2006), Oxygen minimum zone expansion in the eastern tropical North Pacific during deglaciation, *Geophys. Res. Lett.*, *33*, L20602, doi:10.1029/2006GL025975.

Hendy, I. L., T. F. Pedersen, J. P. Kennett, and R. Tada (2004), Intermittent existence of a southern Californian upwelling cell during submillennial climate change of the last 60 kyr, *Paleoceanography*, *19*, PA3007, doi:10.1029/2003PA000965.

Hutchins, D. A., and K. W. Bruland (1998), Iron-limited diatom growth and Si:N uptake ratios in a coastal upwelling regime, *Nature*, *393*, 561–564, doi:10.1038/31203.

Kao, S. J., K. K. Liu, S. C. Hsu, Y. P. Chang, and M. H. Dai (2008), North Pacific–wide spreading of isotopically heavy nitrogen from intensified denitrification during the Bølling/Allerød and post-Younger Dryas periods: Evidence from the western Pacific, *Biogeosci. Discuss.*, *5*, 1017–1033.

Kessler, W. S. (2006), The circulation of the eastern tropical Pacific: A review, *Prog. Oceanogr.*, *69*, 181–217, doi:10.1016/j.pocean.2006.03.009.

Kienast, M., et al. (2006), Eastern Pacific cooling and Atlantic overturning circulation during the last deglaciation, *Nature*, *443*, 846–848, doi:10.1038/nature05222.

Kienast, M., M. F. Lehmann, A. Timmermann, E. Galbraith, T. Bolliet, A. Holbourn, C. Normandeau, and C. Laj (2008), A mid-Holocene transition in the nitrogen dynamics of the western equatorial Pacific: Evidence of a deepening thermocline?, *Geophys. Res. Lett.*, *35*, L23610, doi:10.1029/2008GL035464.

Kienast, S. S., S. E. Calvert, and T. F. Pedersen (2002), Nitrogen isotope and productivity variations along the northeast Pacific margin over the last 120 kyr: Surface and subsurface paleoceanography, *Paleoceanography*, *17*(4), 1055, doi:10.1029/2001PA000650.

Kienast, S. S., M. Kienast, S. Jaccard, S. E. Calvert, and R. François (2006), Testing the silica leakage hypothesis with sedimentary opal records from the eastern equatorial Pacific over the last 150 kyrs, *Geophys. Res. Lett.*, *33*, L15607, doi:10.1029/2006GL026651.

Kienast, S. S., M. Kienast, A. C. Mix, S. E. Calvert, and R. François (2007), Thorium-230 normalized particle flux and sediment focusing in the Panama Basin region during the last 30,000 years, *Paleoceanography*, *22*, PA2213, doi:10.1029/2006PA001357.

Lambeck, K., and J. Chappell (2001), Sea level change through the last glacial cycle, *Science*, *292*, 679–686, doi:10.1126/science.1059549.

Lea, D. W., et al. (2006), Paleoclimate history of Galápagos surface waters over the last 135,000 yr, *Quat. Sci. Rev.*, *25*, 1152–1167, doi:10.1016/j.quascirev.2005.11.010.

Liu, K.-K., and I. R. Kaplan (1989), The eastern tropical Pacific as a source of $^{15}N$-enriched nitrate in seawater off southern California, *Limnol. Oceanogr.*, *34*, 820–830.

Loubere, P. (2000), Marine control of biological production in the eastern equatorial Pacific Ocean, *Nature*, *406*, 497–500, doi:10.1038/35020041.

Loubere, P., F. Mekik, R. Francois, and S. Pichat (2004), Export fluxes of calcite in the eastern equatorial Pacific from the Last Glacial Maximum to present, *Paleoceanography*, *19*, PA2018, doi:10.1029/2003PA000986.

Loubere, P., et al. (2007), Variability in tropical thermocline nutrient chemistry on the glacial/interglacial timescale, *Deep Sea Res., Part II*, *54*, 747–761, doi:10.1016/j.dsr2.2007.01.005.

Lukas, R. (1986), The termination of the equatorial undercurrent in the eastern Pacific, *Prog. Oceanogr.*, *16*, 63–90, doi:10.1016/0079-6611(86)90007-8.

Marchitto, T. M., et al. (2007), Marine radiocarbon evidence for the mechanism of deglacial atmospheric $CO_2$, *Science*, *316*, 1456–1459, doi:10.1126/science.1138679.

Martin, J. H., et al. (1991), The case for iron, *Limnol. Oceanogr.*, *36*(8), 1793–1802.

Martinez, P., and R. S. Robinson (2009), Increase in water column denitrification during the deglaciation controlled by oxygen demand in the eastern equatorial Pacific, *Biogeosci. Discuss.*, *6*, 5145–5161.

Martinez, P., F. Lamy, R. R. Robinson, L. Pichevin, and I. Billy (2006), Atypical $\delta^{15}N$ variations at the southern boundary of the East Pacific oxygen minimum zone over the last 50 ka, *Quat. Sci. Rev.*, *25*, 3017–3028, doi:10.1016/j.quascirev.2006.04.009.

McGee, D., et al. (2007), Deglacial changes in dust flux in the eastern equatorial Pacific, *Earth Planet. Sci. Lett.*, *257*, 215–230, doi:10.1016/j.epsl.2007.02.033.

Meissner, K. J., E. D. Galbraith, and C. Völker (2005), Denitrification under glacial and interglacial conditions: A physical approach, *Paleoceanography*, *20*, PA3001, doi:10.1029/2004PA001083.

Mix, A. C., et al. (2003), *Southeast Pacific Paleoceanographic Transects*, Tex. A&M Univ., College Station.

Pena, L. D., I. Cacho, P. Ferretti, and M. A. Hall (2008), El Niño–Southern Oscillation–like variability during glacial terminations and interlatitudinal teleconnections, *Paleoceanography*, *23*, PA3101, doi:10.1029/2008PA001620.

Pennington, J. T., et al. (2006), Primary production in the eastern tropical Pacific: A review, *Prog. Oceanogr.*, *69*, 285–317, doi:10.1016/j.pocean.2006.03.012.

Pichat, S., K. W. W. Sims, R. François, J. F. McManus, S. Brown Leger, and F. Albarède (2004), Lower export production during glacial periods in the equatorial Pacific derived from $(^{231}Pa/^{230}Th)_{xs,0}$ measurements in deep-sea sediments, *Paleoceanography*, *19*, PA4023, doi:10.1029/2003PA000994.

Pichevin, L. E., B. C. Reynolds, R. S. Ganeshram, I. Cacho, L. Pena, K. Keefe, and R. M. Ellam (2009), Enhanced carbon pump inferred from relaxation of nutrient limitation in the glacial ocean, *Nature*, *459*, 1114–1118, doi:10.1038/nature08101.

Pride, C., R. Thunell, D. Sigman, L. Keigwin, M. Altabet, and E. Tappa (1999), Nitrogen isotopic variations in the Gulf of California since the last deglaciation: Response to global climate change, *Paleoceanography*, *14*(3), 397–409, doi:10.1029/1999PA900004.

Robinson, R. S., B. G. Brunelle, and D. M. Sigman (2004), Revisiting nutrient utilization in the glacial Antarctic: Evidence from a new diatom-bound N isotopic analysis, *Paleoceanography*, *19*, PA3001, doi:10.1029/2003PA000996.

Robinson, R. S., D. M. Sigman, P. J. DiFiore, M. M. Rohde, T. A. Mashiotta, and D. W. Lea (2005), Diatom-bound $^{15}N/^{14}N$: New support for enhanced nutrient consumption in the ice age subantarctic, *Paleoceanography*, *20*, PA3003, doi:10.1029/2004PA001114.

Robinson, R. S., et al. (2007), Southern Ocean control on the extent of denitrification in the southeast Pacific over the last 70 ka, *Quat. Sci. Rev.*, *26*, 201–212, doi:10.1016/j.quascirev.2006.08.005.

Sholkovitz, E. R., et al. (1999), Island weathering: River sources of rare earth elements to the western Pacific Ocean, *Mar. Chem.*, *68*(1–2), 39–57, doi:10.1016/S0304-4203(99)00064-X.

Siddall, M., et al. (2003), Sea-level fluctuations during the last glacial cycle, *Nature*, *423*, 853–858, doi:10.1038/nature01690.

Sigman, D. M., M. A. Altabet, D. C. McCorkle, R. Francois, and G. Fischer (2000), The $\delta^{15}N$ of nitrate in the Southern Ocean: Nitrogen cycling and circulation in the ocean interior, *J. Geophys. Res.*, *105*(C8), 19,599–19,614, doi:10.1029/2000JC000265.

Spero, H. J., and D. W. Lea (2002), The cause of carbon isotope minimum events on glacial terminations, *Science*, *296*, 522–525, doi:10.1126/science.1069401.

Takeda, S. (1998), Influence of iron availability on nutrient consumption ratio of diatoms in oceanic waters, *Nature*, *393*, 774–777, doi:10.1038/31674.

Toggweiler, J. R., and S. Carson (1995), What are the upwelling systems contributing to the ocean's carbon and nutrient budgets?, in *Upwelling in the Ocean: Modern Processes and Ancient Records*, edited by C. P. Summerhayes et al., pp. 337–360, John Wiley, New York.

Toggweiler, J. R., K. Dixon, and W. S. Broecker (1991), The Peru upwelling and the ventilation of the South-Pacific thermocline, *J. Geophys. Res.*, *96*(C11), 20,467–20,497, doi:10.1029/91JC02063.

Wells, M. L., G. K. Vallis, and E. A. Silver (1999), Tectonic processes in Papua New Guinea and past productivity in the eastern equatorial Pacific Ocean, *Nature*, *398*, 601–604, doi:10.1038/19281.

Winckler, G., R. F. Anderson, M. Q. Fleisher, D. McGee, and N. Mahowald (2008), Covariant glacial-interglacial dust fluxes in the equatorial Pacific and Antarctica, *Science*, *320*, 93–96, doi:10.1126/science.1150595.

Ziegler, C. L., R. W. Murray, T. Plank, and S. R. Hemming (2008), Sources of Fe to the equatorial Pacific Ocean from the Holocene to Miocene, *Earth Planet. Sci. Lett.*, *270*, 258–270, doi:10.1016/j.epsl.2008.03.044.

I. Cacho and L. D. Pena, GRC Geociències Marines, Department of Stratigraphy, Paleontology and Marine Geosciences, University of Barcelona, C/ Martí Franques, s/n E-08028 Barcelona, Spain.

P. Martinez, EPOC, UMR 5805, Université Bordeaux 1, CNRS, Avenue des Facultés, F-33405 Talence CEDEX, France.

R. S. Robinson, Graduate School of Oceanography, University of Rhode Island, Narragansett, RI 02882, USA. (rebeccar@gso.uri.edu)